View metadata, citation and similar papers at core.ac.uk
brought to you by CORE
provided by PolyU Institutional Repository

Can Young's modulus and hardness of wire structural materials be directly measured using nanoindentation?

S.Q. Shu, Y. Yang, T. Fu, C.S. Wen, and J. Lu[a)]
Department of Mechanical Engineering, the Hong Kong Polytechnic University, Hung Hom, Kowloon, Hong Kong, China

(Received 28 July 2008; accepted 12 November 2008)

In recent studies, nanoindentation experiments combined with the Oliver and Pharr method (OP method) are frequently used to measure the mechanical properties of "one-dimensional" structural materials (micro/nanowires and nanobelts) regardless of the corresponding assumptions of the OP method. This article reports the numerical simulation studies of the nanoindentations of wire structural materials on elastic-plastic substrates using dimensional analysis and the finite element method. We find that the measured hardness and Young's modulus of wire structural materials are significantly influenced by their geometries and indenters as well as the mechanical properties of substrates and wires.

I. INTRODUCTION

Over the past decades, one-dimensional (1D) structural materials (such as micro/nanowires and nanobelts) have attracted the attention of scientists for their excellent properties and broad potential applications. For their applications, obtaining the mechanical behaviors of the 1D structural materials is the key step when they are integrated into advanced products. In recent studies, nanoindentation experiments combined with the Oliver and Pharr method (OP method) are frequently used to study the mechanical properties of 1D structural materials, especially properties of the 1D nanostructural materials (nanowires and nanobelts), because their mechanical properties are obtained with difficulty using the conventional testing instruments and techniques for their tiny volumes, sample clamping requirement, and super measuring precision.[1–6]

A significant reduction in the measured Young's moduli of the aluminum borate ($Al_4B_2O_9$ and $Al_{18}B_4O_3$) nanowires, in the range of 50 to 70%, compared with those of the bulk materials was reported using nanoindentation with the OP method, which was then attributed to the loss of constraints on surface atoms.[4] The low Young's modulus, compared with the counterpart bulk materials, was also observed in other nanowires, such as ZnO, ZnS, and GaN.[1,7,8] In contrast, nanoindentation of gold and silver nanowires yielded the Young's moduli comparable with those of the bulk materials.[2,3] However, according to atomic simulations, the nanowires have a comparable Young's modulus with that of the corresponding bulk material, and the surface and edge effects of nanowires can be negligible when the diameters of the nanowires are larger than 3 to 4 nm.[9] Meanwhile, using the surface stress theory, the divergences between the Young's modulus of ZnO nanowires and those of the bulk materials are small (in the range of 10%) and decrease as the diameter increases, when their diameters are larger than 50 nm.[10] The apparent discrepancies between different experiments and analysis indicate that the physics and mechanics of wire structural materials underlying the foregoing experiments may not be fully explored and therefore need further investigations.

In this study, three-dimensional (3D) finite element simulations (FEM) and dimensional analysis are performed to study the nanoindentation of wire structural materials, which mechanical properties are comparable with the corresponding bulk materials, on an elastic-plastic substrate by a cone indenter. For deviating from the original assumptions of the Oliver and Pharr method, the effect factors (the geometries of wire structural materials and indenter and the mechanical properties of wire structural materials and substrates) on the measured hardness and Young's modulus of wire structural materials from the Oliver and Pharr method are investigated in detail; in addition, the applicability of the Oliver and Pharr method on the mechanical property measurement of wire structural materials is investigated.

II. MODELING AND ANALYSES

The Oliver and Pharr method was originally developed to study the hardness and Young's modulus of bulk elastic-plastic materials. That is, below the initial yield stress, σ_Y, the materials are elastic and can be characterized with the Young's modulus, E, and Poisson's ratio, ν. After yielding, the stress-strain curves of

[a)]Address all correspondence to this author.
e-mail: Jian.Lu@inet.polyu.edu.hk
DOI: 10.1557/JMR.2009.0079

 © 2009 Materials Research Society
http://journals.cambridge.org Downloaded: 04 Oct 2013 IP address: 158.132.161.103

the materials can be described with the strain hardening exponent, n, and the following relationship:

$$\sigma = \sigma_Y (E\varepsilon/\sigma_Y)^n \quad . \tag{1}$$

In the present study, the mechanical behaviors of elastic-plastic wire structural materials are characterized with E_w, v_w, σ_{Yw}, and n_w, whereas the mechanical properties of substrate and indenter are characterized with E_s, v_s, σ_{Ys} and E_i, v_i, respectively.

A typical indentation curve obtained with a conical indenter is presented in Fig. 1, which is composed of loading and unloading curves. In addition, it is assumed that elastic-plastic deformation occurs during loading, but that elastic deformation only occurs during unloading. Based on the unloading curve of indentation and the Oliver and Pharr method, the hardness, H_B^{OP}, and the reduced Young's modulus, E_B^{OP}, of the elastic-plastic bulk materials can be obtained with the OP method using the following formulas[11]:

$$H_B^{OP} = \frac{P_{\max}}{A(h_c)} \quad , \tag{2}$$

$$E_B^{OP} = \frac{\sqrt{\pi}}{2\beta} \frac{S}{\sqrt{A(h_c)}} \quad , \tag{3}$$

where $P_{\max}$ denotes the maximum indentation load; $A(h_c)$ is the corresponding projected area of contact area related to the contact depth h_c; β is a correction factor; and S denotes the initial slope of the unloading curve $\left(= \frac{dP}{dh}\big|_{h=h_{\max}}\right)$. The mark "*op*" stands for the physical quantities that can be extracted from the *P-h* curves using the Oliver and Pharr method, and the subscript "*B*" stands for the bulk elastic-plastic materials.

In the article, the 3D conical indenter modeled with the tip radius, R', and the tip half angle, θ, is adopted to study the nanoindentations of wire structural materials. Based on the Oliver and Pharr method, for indentation depths much larger than the indenter tip radius ($h \gg R'$), according to dimensional analysis, the indentation hardness and Young's modulus of bulk materials with the same mechanical properties of wire structural materials can be written as[9–12]:

$$\frac{H_B^{OP}}{\sigma_{Yw}} = \Pi_1 \left(\frac{E_r}{\sigma_{Yw}}, n_w; \theta \right) \quad , \tag{4}$$

$$\frac{E_B^{OP}}{\sigma_{Yw}} = \Pi_2 \left(\frac{E_r}{\sigma_{Yw}}, n_w; \theta \right) \quad . \tag{5}$$

Note that, in deriving Eqs. (4) and (5), the contact friction, f_1, between the indenter and the indented material is neglected in the Oliver and Pharr method. In addition, E_r is the reduced Young's modulus, which accounts for the mutual elastic deformation during indentation, given as follows:

$$E_r = \left(\frac{1 - v_w^2}{E_w} + \frac{1 - v_i^2}{E_i} \right)^{-1} \quad . \tag{6}$$

For the nanoindentations of wire structural materials, the wire structural materials can be modeled as the length, l, and the radius, R, which are comparable with the radius of indenter; in addition, the indentation of wire structural materials on an elastic-perfectly plastic substrate entails two contacts, as depicted in inset I of Fig. 2. Based on the Oliver and Pharr method, the new length-scale parameters that are related to the geometries of wire structural materials and indenters and the mechanical properties of substrates enter the dimensional equations, i.e., Eqs. (4) and (5), which give:

$$\frac{H_w^{OP}}{\sigma_{Yw}} = \Pi_3 \left(\frac{E_r}{\sigma_{Yw}}, n_w; \frac{\sigma_{Yw}}{\sigma_{Ys}}, \frac{E_r}{E_{rs}}; f_1, f_2, \frac{l}{R}, \frac{R'}{R}, \frac{h}{R}, \theta \right) \quad , \tag{7}$$

$$\frac{E_w^{OP}}{\sigma_{Yw}} = \Pi_4 \left(\frac{E_r}{\sigma_{Yw}}, n_w; \frac{\sigma_{Yw}}{\sigma_{Ys}}, \frac{E_r}{E_{rs}}; f_1, f_2, \frac{l}{R}, \frac{R'}{R}, \frac{h}{R}, \theta \right) \quad . \tag{8}$$

Note that, in deriving Eqs. (7) and (8), the friction coefficients f_1 and f_2 among the indenter, wire structural materials, and substrate are taken to be 0.1 to account for the limited tangential adhesion among them and then omitted.[13]

The subscript "*w*" stands for the wire structural materials. In addition, H_w^{OP} and E_w^{OP} are the hardness and Young's modulus, respectively, of the wire structural materials from the Oliver and Pharr method; E_{rs} is the reduced Young's modulus, which accounts for the mutual elastic deformation between the nanowire and the substrate, which is:

$$E_{rs} = \left(\frac{1 - v_w^2}{E_w} + \frac{1 - v_s^2}{E_s} \right)^{-1} \quad , \tag{9}$$

where the script '*s*' denotes the substrate and the other symbols have their usual meanings. According to

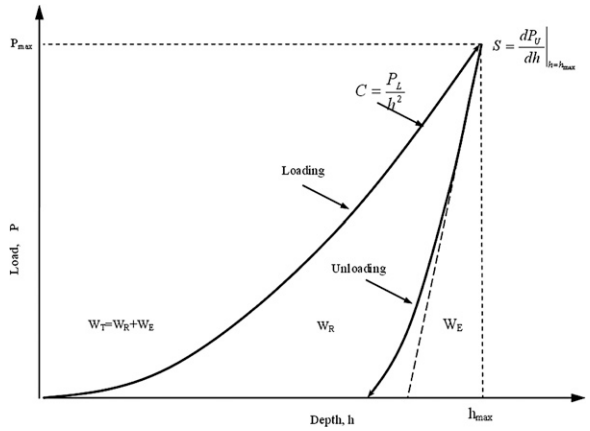

FIG. 1. Schematic illustration of the indentation load-depth data of elastic-plastic bulk materials indented by a sharp indenter.

CAMBRIDGE JOURNALS
http://journals.cambridge.org Downloaded: 04 Oct 2013 IP address: 158.132.161.103

Eqs. (4), (5), (7), and (8), the following relationships can be further obtained:

$$\frac{H_w^{OP}}{H_B^{OP}} = \Pi_5\left(\frac{E_r}{\sigma_{Yw}}, n_w; \frac{\sigma_{Yw}}{\sigma_{Ys}}, \frac{E_r}{E_{rs}}; \frac{l}{R}, \frac{R'}{R}, \frac{h}{R}, \theta\right) \quad , \quad (10)$$

$$\frac{E_w^{OP}}{E_B^{OP}} = \Pi_6\left(\frac{E_r}{\sigma_{Yw}}, n_w, \frac{\sigma_{Yw}}{\sigma_{Ys}}, \frac{E_r}{E_{rs}}; \frac{l}{R}, \frac{R'}{R}, \frac{h}{R}, \theta\right) \quad . \quad (11)$$

The 3D indentation model and geometry are adopted to depict the nanoindentations of wire structural materials in Fig. 2. The symmetry of the model (1/4 symmetry) can be realized by examining the symmetry of nanowire under the given boundary conditions. The left cross-section of nanowire is fixed in the Z direction, the right end of nanowire is fixed in all directions, and the inner surface is fixed in the X directions; whereas the down surface of substrate are fixed in all directions, the left cross-section of substrate is fixed in the Z direction, and the inner surface of substrate is fixed in the X direction. At the same time, the indenter can be only moved in the direction of Y direction. For the bulk materials, the details of the finite element model have been given previously.[14]

Because there are no analytical solutions to the problem of conical indentations in elastic-plastic wire structural materials, a 3D finite element model was invoked with the commercial FEM package ABAQUS (HKS Inc., Pawtucket, RI)[15] to systematically investigate the dimensionless functions Eqs. (10) and (11). In addition, the four-node 3D continuum elements were used to mesh the contact system. As shown in Fig. 2, insets II and III, the mesh was refined in the contact area as opposed to the coarse mesh far away, providing a good compromise between the computational accuracy and cost. In the simulation, the model assumed isotropic power-law strain hardening, the yield criterion was that of Von Mises, and large deformation formulations were included. In addition, the convergence of the numerical solutions has been proved with 15,200 elements.

In the numerical simulations, the cone rigid indenter with a half-included angle of 70.3°, which is equivalent to a Berkovich indenter, is adopted. In addition, l/R was taken as 30 because the relative errors of the simulated results were within 5% when $l/R \geq 30$ according to the numerical simulations.

To evaluate the dependence of the normalized Young's modulus and hardness of nanowires on the $\frac{E_r}{\sigma_{Yw}}$ and n_w, we take the substrate as a rigid body, the tip radius of the sharp cone rigid indenter, R', as 0, and the indenting depth as six-tenths of wire's radius, R, as illustrated in Fig. 2. That is, $\frac{\sigma_{Yw}}{\sigma_{Ys}} \to 0, \frac{E_r}{E_{rs}} \to 1, \frac{R'}{R} = 0, \frac{h}{R} = 0.6$ in Eqs. (10) and (11). In Fig. 3, the results from the finite element studies show to what extent H_w^{OP}/H_B^{OP} and E_w^{OP}/E_B^{OP} depend on $\frac{E_r}{\sigma_{Yw}}$, n_w. Compared with those of normalized hardness, the divergences of the normalized Young's modulus' errors caused by the two properties of $\frac{E_r}{\sigma_{Yw}}$ and n_w are larger. In addition, the smaller the $\frac{E_r}{\sigma_{Yw}}$ and n_w values, the larger the errors of normalized Young's modulus.

To study the effects of elastic-plastic deformations of the substrates on the normalized hardness and Young's modulus of wire structural materials, a series of wire-substrate systems with $0.01 \leq \frac{\sigma_{Ys}}{\sigma_{Yw}} \leq 10$ and $0 < \frac{E_w}{E_s} \leq 10$, which are decided by E_r/E_{rs} according to Eq. (9), are studied for the given normalized indentation depths, $\frac{h}{R} = 0.6$. In the simulations, the wire structural materials have the mechanical properties of $\frac{E_w}{\sigma_{Yw}} = 100$, $n_w = 0.1$;

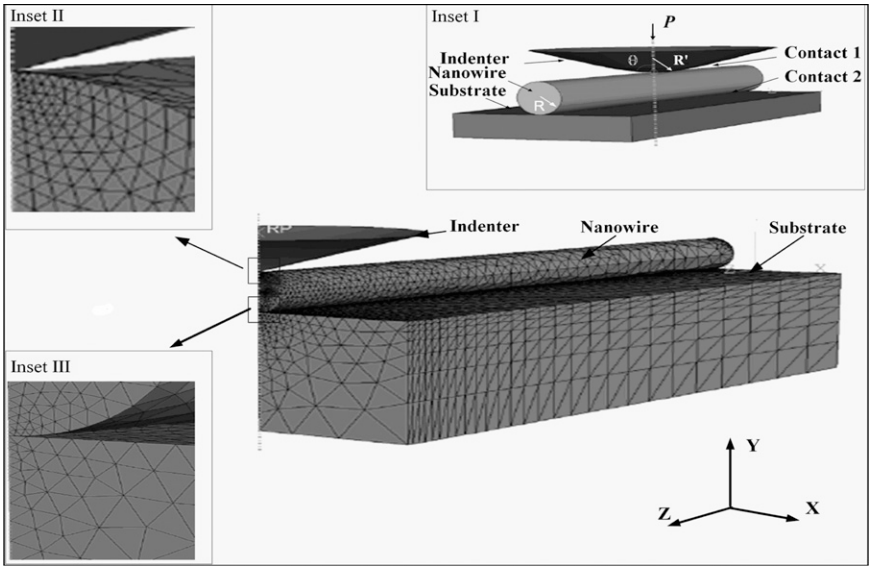

FIG. 2. Schematic of the contact geometries and the 3D finite element model of the indentation of a nanowire on an elastic-plastic substrate.

http://journals.cambridge.org Downloaded: 04 Oct 2013 IP address: 158.132.161.103

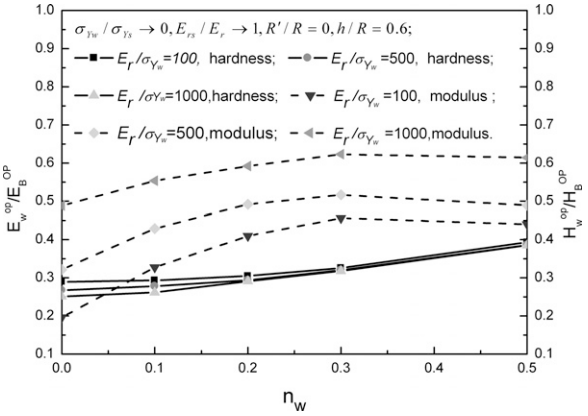

FIG. 3. The normalized hardness and Young's modulus of nanowires versus mechanical properties of $\frac{E_r}{\sigma_{Yw}}$ and n_w for the rigid substrates, the given geometries of wires, and the perfectly sharp cone rigid indenters.

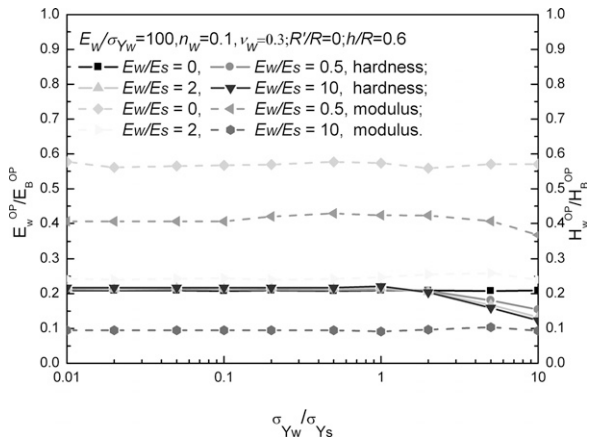

FIG. 4. The normalized hardness and Young's modulus of nanowires versus the mechanical properties of E_w/E_s and σ_{Yw}/σ_{Ys} for the given mechanical properties and geometries of wires, and the perfectly sharp cone rigid indenters.

in addition, the radius of indenter, R', is taken as 0 (that is, $R'/R = 0$). On the one hand, the numerical results in Fig. 4 show that for the studied wire-substrate systems with given $\frac{E_w}{E_s}$, the effects of $\frac{\sigma_{Yw}}{\sigma_{Ys}}$ on normalized hardness and Young's modulus are neglected when $\frac{\sigma_{Yw}}{\sigma_{Ys}} \leq 1$, whereas the effects are large when $\frac{\sigma_{Yw}}{\sigma_{Ys}} > 1$. On the other hand, the divergences of normalized Young's modulus caused by the varieties of $\frac{E_w}{E_s}$ are larger than those of the normalized hardness for the wire-substrate systems with the given $\frac{\sigma_{Ys}}{\sigma_{Yw}}$. In addition, the larger the $\frac{E_w}{E_s}$ values, the smaller the normalized Young's modulus. According to the study, the elastic-plastic deformations of substrates greatly affect the measured value of hardness and Young's modulus of wire structural materials.

In this study, our analysis is further focused on the geometry effects (the radius of indenter tip, the radius of wire structural materials, and indentation depth) on the measured hardness and Young's modulus of wire

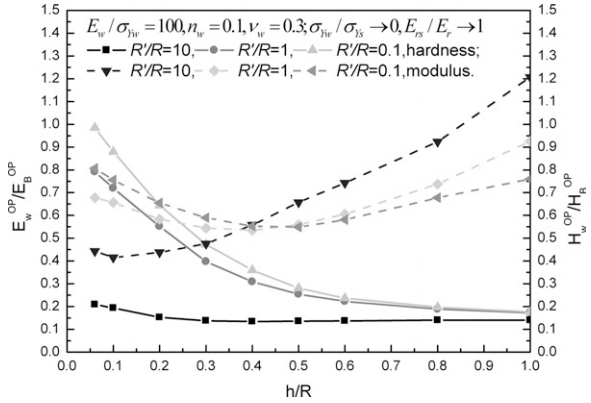

FIG. 5. The normalized hardness and Young's modulus as a function of the normalized indent depth, h/R, for different normalized rigid indenter tip radii for the given mechanical properties of wires and substrates, and the given geometries of wires.

structural materials on rigid substrates. In Fig. 5, the values of normalized hardness of wire structural materials are significantly underestimated, especially in cases where the indenter tip radius is larger than that of a wire; for example, the normalized hardness of wire structural materials is equal to 0.4 for $R'/R = 1$ and $h/R = 0.3$. In contrast, the normalized Young's modulus of wire structural materials initially decreases with the increasing normalized indent depth, h/R, and then increases with the increasing normalized indent depth after it passes a critical value (Fig. 5). The descending trend observed in the shallow indent regime is attributed to the curvature effect of nanowires, which is not accounted for in the Oliver and Pharr method. Because the indenter tip radius and indent depth are much smaller than the wire radius, the deviation from the contact geometries in the Oliver and Pharr method is, to some degree, remedied, the extracted wire structural materials' Young's modulus should be equal to the value of the corresponding bulk material. However, the substrate effect emerges as the indenter penetrates deeply into the wire structural materials, which results in the ascending trend observed in the deep indent regime. Please note that the divergence in the extracted Young's modulus of wire structural materials at deep indent depths is caused by the rigid body assumption for the substrate ($E_s \to \infty$).

III. CONCLUSION

In summary, for the wire structural materials with 10-nm diameters or more and generally have comparable mechanical behaviors with those of the corresponding bulk materials,[9,10] the hardness and Young's modulus from nanoindentations using the Oliver and Pharr method without corrections may be significantly underestimated regardless of the effects of the geometries of wire structural materials and the indenter and the mechanical

CAMBRIDGE JOURNALS
http://journals.cambridge.org Downloaded: 04 Oct 2013 IP address: 158.132.161.103

behaviors of wire structural materials and substrates. Moreover, for the nanowires with 10-nm diameters or less, the size effects caused by the inner physical mechanism of micromaterials, which are out of the scope of this paper, also affect the measurement of their mechanical properties and will be addressed in our future work. Therefore, a more robust and reliable measurement that can be used to study the mechanical properties of wire structural materials is needed in the future.

ACKNOWLEDGMENTS

The authors would like to thank the reviewers for their constructive and helpful comments, and acknowledge the financial support of the Research Grant Council of the Hong Kong SAR under the project PolyU 5189/07E (GRF) and the Hong Kong Polytechnic University funds for niche areas under Grant No. BB90.

REFERENCES

1. S.X. Mao, M. Zhao, and Z.L. Wang: Nanoscale mechanical behavior of individual semiconducting nanobelts. *Appl. Phys. Lett.* **83,** 993 (2003).
2. X.D. Li, P. Nardi, C.W. Baek, J.M. Kim, and Y.K. Kim: Direct nanomechanical machining of gold nanowires using a nanoindenter and an atomic force microscope. *J. Micromech. Microeng.* **15,** 551 (2005).
3. X.D. Li, H.S. Gao, C.J. Murphy, and K.K. Caswell: Nanoindentation of silver nanowires. *Nano Lett.* **3,** 1495 (2003).
4. X.Y. Tao, X.N. Wang, and X.D. Li: Nanomechanical characterization of one-step combustion-synthesized $Al_4B_2O_9$ and $Al_{18}B_4O_{33}$ nanowires. *Nano Lett.* **7,** 3172 (2007).
5. X.Y. Tao and X.D. Li: Catalyst-free synthesis, structural, and mechanical characterization of twinned $Mg_2B_2O_5$ nanowires. *Nano Lett.* **8,** 505 (2008).
6. H. Ni and X. Li: Synthesis, structural and mechanical characterization of amorphous and crystalline boron nanobelts. *J. Nano Res.* **1,** 10 (2008).
7. H. Ni, X.D. Li, G.S. Cheng, and R. Klie: Mechanical properties of single-crystal GAN nanowires. *J. Mater. Res.* **21,** 2882 (2006).
8. G. Feng, W.D. Nix, Y. Yoon, and C.J. Lee: A study of the mechanical properties of nanowires using nanoindentation. *J. Appl. Phys.* **99,** 074304 (2006).
9. J. Diao, K. Gall, and M.L. Dunn: Atomistic simulation of the structure and elastic properties of gold nanowires. *J. Mech. Phys. Solids* **52,** 1935 (2004).
10. G.F. Wang and X.D. Li: Size dependency of the elastic modulus of ZnO nanowires. *Appl. Phys. Lett.* **91,** 1 (2007).
11. W.C. Oliver and G.M. Pharr: An improved technique for determining hardness and elastic modulus. *J. Mater. Res.* **7,** 1564 (1992).
12. Y.T. Cheng and C.M. Cheng: Scaling, dimensional analysis, and indentation measurements. *Mater. Sci. Eng., R* **44,** 91 (2004).
13. M. Mata and J. Alcala: The role of friction on sharp indentation. *J. Mech. Phys. Solids* **52,** 145 (2004).
14. S.Q. Shu, J. Lu, and D.F. Li: A systematic study of the validation of Oliver and Pharr's method. *J. Mater. Res.* **22,** 3385 (2007).
15. ABAQUS, version 6.6 (Hibbit, Karlson & Sorensen, Inc., Pawtucket, RI).

http://journals.cambridge.org Downloaded: 04 Oct 2013 IP address: 158.132.161.103